Redoxal, an Inhibitor of De Novo Pyrimidine Biosynthesis, Augments APOBEC3G Antiviral Activity Against Human Immunodeficiency Virus Type 1

Erez Pery[1,2], **Ann Sheehy**[4], **N. Miranda Nebane**[5], **Vikas Misra**[1], **Marie K. Mankowski**[6], **Lynn Rasmussen**[5], **E. Lucile White**[5], **Roger G. Ptak**[6], and **Dana Gabuzda**[1,3,*]

[1]Department of Cancer Immunology and AIDS, Dana Farber Cancer Institute, Boston, Massachusetts 02115

[2]Department of Pathology, Harvard Medical School, Boston, Massachusetts 02115

[3]Department of Neurology (Microbiology), Harvard Medical School, Boston, Massachusetts 02115

[4]Department of Biology, College of the Holy Cross, Worcester, MA 01610

[5]Southern Research Institute High Throughput Screening Center, Birmingham, AL 35205

[6]Southern Research Institute, Department of Infectious Disease Research, Frederick, MD 21701

Abstract

APOBEC3G (A3G) is a cytidine deaminase that restricts HIV-1 replication by inducing G-to-A hypermutation in viral DNA; deamination-independent mechanisms are also implicated. HIV-1 Vif protein counteracts A3G by inducing its proteasomal degradation. Thus, the Vif-A3G axis is a potential therapeutic target. To identify compounds that inhibit Vif:A3G interaction, a 307,520 compound library was tested in a TR-FRET screen.. Two identified compounds, redoxal and lomofungin, inhibited HIV-1 replication in peripheral blood mononuclear cells. Lomofungin activity was linked to A3G, but not pursued further due to cytotoxicity. Redoxal displayed A3G-dependent restriction, inhibiting viral replication by stabilizing A3G protein levels and increasing A3G in virions. A3G-independent activity was also detected. Treatment with uridine or orotate, intermediates of pyrimidine synthesis, diminished redoxal-induced stabilization of A3G and antiviral activity. These results identify redoxal as an inhibitor of HIV-1 replication and suggest its ability to inhibit pyrimidine biosynthesis suppresses viral replication by augmenting A3G antiviral activity.

*Corresponding Author: Dr. Dana Gabuzda, CLS 1010, 450 Brookline Avenue, Boston, MA, 02215, Tel: (617)-632-2154; dana_gabuzda@dfci.harvard.edu.

Keywords

HIV-1; Vif; APOBEC3G; antiviral; redoxal; pyrimidine synthesis

BACKGROUND

While current antiretroviral therapies prolong the lifespan of people living with HIV/AIDS, they fail to completely clear the virus reservoir, resulting in a chronic infection (Ketseoglou et al., 2014; Kumar et al., 2014; Li et al., 2012). These antiretroviral regimens also have significant side effects, including lipodystrophy, hyperglycemia, renal dysfunction, osteoporosis, and cardiovascular disease (Carr and Cooper, 2000; Kalayjian et al., 2012; Max and Sherer, 2000; Towner et al., 2012). Due to side effects as well as the common problem of drug resistance, novel antiretrovirals are needed to offer new treatment options. With exception of CCR5 antagonists and other entry inhibitors, current HIV-1 drug regimens only target the viral enzymes.

A3G, a cellular antiviral restriction factor, and its viral antagonist Vif (viral infectivity factor) have recently emerged as attractive targets for novel anti-HIV-1 therapeutics (Aires da Silva et al., 2004; Goncalves et al., 2002; Malim and Bieniasz, 2012; Smith et al., 2009; Strebel, 2013). A3G is a member of the APOBEC3 (A3) family of single-stranded (ss) DNA cytidine deaminases that serve as critical post-entry barriers to retroviral replication (Esnault et al., 2005; Esnault et al., 2006; Harris et al., 2003; Mangeat et al., 2003). All A3 family members (A3A, A3B, A3C, A3D, A3F, A3G, and A3H) have known antiviral activity (Goila-Gaur and Strebel, 2008; Malim, 2009). A common feature characterizing the A3 family is the presence of a catalytic domain composed of a conserved zinc-binding motif, which catalyzes the hydrolytic deamination of deoxycytidine, converting it to deoxyuridine (Wang et al., 2011).

A3G is a potent antiretroviral host factor widely expressed in hematopoietic cells, including CD4+ T cells and myeloid cells (Bonavia et al., 2011). In the absence of a functional Vif protein, A3G protein is incorporated into HIV-1 virions and deaminates cytidine to uridine in the viral minus-strand DNA during reverse transcription, resulting in G-to-A hypermutation and premature degradation of newly synthesized viral DNA (Harris et al., 2003; Mangeat et al., 2003; Miyagi et al., 2007; Schumacher et al., 2008; Zhang et al., 2003). A3G has also been shown to inhibit HIV-1 replication via deamination-independent mechanisms (Belanger et al., 2013; Bishop et al., 2006; Chaurasiya et al., 2014; Gillick et al., 2013; Guo et al., 2007; Holmes et al., 2007; Luo et al., 2007; Newman et al., 2005).

HIV-1 and other lentiviruses overcome this antiviral activity of A3G via the viral accessory protein Vif. Vif binds to A3G prior to its incorporation into virions and induces its ubiquitination and degradation via the 26S proteasome. Vif must also associate with the core-binding factor subunit beta (CBF-β) and Cullin 5 (Cul5)-EloB-EloC E3 ligase complex to exert its anti-A3G effects through proteasomal degradation pathways (Guo et al., 2014; Jager et al., 2012; Wang et al., 2013). Vif may also inhibit A3G through mechanisms independent of proteasomal degradation (Kao et al., 2003; Kao et al., 2004). Small molecules that inhibit HIV-1 Vif function *in vitro* have been identified, but these compounds

do not inhibit the Vif-A3G interaction (Cen et al., 2010; Matsui et al., 2014; Nathans et al., 2008; Pan et al., 2015; Zuo et al., 2012).

In a recent study (Pery et al., 2015), we reported using a high-throughput screen (HTS) for inhibitors of the Vif-A3G interaction and identification of a novel compound N.41 that attenuates HIV-1 replication by liberating A3G from Vif regulation, leading to an increase in its innate antiviral activity. Here, we report two additional compounds identified in the HTS, lomofungin and redoxal, which exhibit potent antiviral activity against HIV-1 replication in PBMCs. Unexpectedly, we found that redoxal, a known inhibitor of the *de novo* pyrimidine biosynthesis pathway, attenuates HIV-1 replication by stabilizing the A3G protein, increasing its incorporation into virions and thereby augmenting its innate antiviral activity. Antiviral activity independent of A3G was also detected.

RESULTS

Identification of redoxal and lomofungin as inhibitors of Vif-A3G interaction

To identify compounds that inhibit the interaction between HIV-1 Vif and A3G, we used a homogeneous time-resolved fluorescence resonance energy transfer (TR-FRET) high-throughput screening assay (Fig. 1A) (Mehle et al., 2007; Pery et al., 2009; Pery et al., 2015). In this assay, interaction between a purified GST-Vif protein fragment that includes the A3G binding site (1–94 amino acids; GST-Vif) (Dang et al., 2010a; Dang et al., 2010b; Kouno et al., 2015; Mehle et al., 2007; Pery et al., 2009; Russell and Pathak, 2007; Yamashita et al., 2008), and a synthetic biotinylated A3G peptide corresponding to amino acids 110–148, which encompasses the Vif-binding site (Bogerd et al., 2004; Huthoff and Malim, 2007; Mangeat et al., 2004; Schrofelbauer et al., 2004), is detected by Europium (Eu-donor fluorophore)-labeled anti-GST antibodies and Streptavidin-Ulight (acceptor fluorophore). Interaction between Vif and A3G brings Eu and Ulight into close proximity, supporting energy transfer between these molecules; this energy transfer is then measured as a FRET signal and attenuation of Vif-A3G interaction results in signal reduction.

A 307,520 compound library was screened and active hits were identified as described (Pery et al., 2015). The complete results of the HTS can be found at Pubchem under AID 1117320 (https://pubchem.ncbi.nlm.nih.gov/assay/assay.cgi?aid=1117320). The secondary TR-FRET-based dose-response assay and counter screens for specificity validated redoxal and lomofungin as promising compounds for subsequent evaluation (Fig. 1B). Lomofungin, a natural product compound first isolated from the soil-dwelling Gram-positive bacteria *Streptomyces lomodensis*, was previously shown to inhibit RNA synthesis in yeast, fungi, and Gram-positive and Gram-negative bacteria (Cano et al., 1973; Johnson and Dietz, 1969; Klo et al., 1973). Lomofungin was subsequently identified as an inhibitor of botulinum neurotoxin light chain protease (Eubanks et al., 2010) and as a potential therapeutic for myotonic dystrophy type 1 (Hoskins et al., 2014a). Redoxal is a synthetic compound originally identified by a computer algorithm as an inhibitor of dihydroorotate dehydrogenase (DHODH), an essential enzyme in the *de novo* pyrimidine synthesis pathway (Fig. 1C) (Cleaveland et al., 1995; Knecht and Loffler, 2000). Redoxal inhibits pyrimidine biosynthesis through this mechanism, and was previously shown to inhibit DHODH in

Candida albicans and exert antiviral activity against West Nile virus (Chung et al., 2010; Zameitat et al., 2006).

Redoxal and lomofungin inhibit HIV-1 replication in PBMCs

The next step in our screening pipeline included a cell-based assay to identify compounds that attenuate Vif-dependent degradation of A3G in 293T cells and an assay testing antiviral activity in PBMCs. Although redoxal and lomofungin had little effect on Vif-dependent degradation of A3G in the YFP-A3G assay, these compounds had strong antiviral activity when tested against HIV-1 replication in PBMCs. Redoxal had an IC_{50} as low as 1.37 μM and TC_{50} >100 μM, while lomofungin had an IC_{50} as low as 0.07 μM and TC_{50} = 3.6 μM when tested against HIV-1$_{Ba-L}$ replication in PBMCs (Fig. 2A). However, further examination of lomofungin antiviral activity revealed a low therapeutic index (TI_{50}) in PBMCs due to its cytotoxicity (data not shown).

Further testing of lomofungin and compound analogs

The antiviral activity of lomofungin was further examined by testing its effects on HIV-1$_{NL4-3}$ replication in H9 (A3G-expressing; A3G+) and SupT1 (A3G-negative; A3G−) T cells. At 62.5 and 125 nM, lomofungin demonstrated strong antiviral activity in H9 cells expressing A3G but not in SupT1 T cells lacking A3G expression, but concentrations greater than 125 nM caused significant cytotoxicity in both cell lines (Additional File 1). To address and potentially ameliorate this cell toxicity, lomofungin analogs were identified and tested for viral suppression and cytotoxicity in PBMCs (Additional Files 2 and 3). The most promising analog, Analog 4, showed no significant cytotoxicity but had an IC_{50} range of 17.8–24.3 μM when tested against replication of several HIV-1 isolates, indicating weak antiviral activity. Therefore, further studies of lomofungin were not pursued.

Redoxal exhibits A3G-dependent antiviral activity against diverse HIV-1 isolates

Next, we further examined the antiviral activity of redoxal. First, we tested its antiviral activity against the HIV-1 isolates 89BZ167 and 91US001, which demonstrated IC_{50}s of 0.59 and 1.74 μM, respectively, and confirmed the antiviral activity against BaL (IC_{50} of 2.94 μM) shown in preceding experiments (Fig. 2B). Therapeutic index values for redoxal ranged from >34 to >168, while AZT, included as a positive control, displayed a therapeutic index ranging from >225->395 (Fig. 2B). To evaluate A3G-dependent antiviral activity, redoxal was tested for its ability to suppress HIV-1$_{NL4-3}$ replication in spreading infections in non-permissive CEM cells that express high levels of A3G and other APOBEC3 proteins, and in permissive CEM-SS cells, a subclone of CEM cells that expresses very low levels of A3G and other APOBEC3 proteins (Fig. 3A) (Refsland et al., 2010). Redoxal treatment inhibited viral replication in a dose-dependent manner in CEM cells but not CEM-SS cells, suggesting A3G-dependent antiviral activity. To further characterize dependence on A3G, we examined A3G and Vif protein levels in redoxal-treated cells by Western blotting of cell lysates at 3 and 6 days post infection (Fig. 3B). Treatment with 1250 nM redoxal reduced Vif protein levels in CEM cells, while A3G protein levels showed a modest increase at 6 days post infection. High molecular weight (HMW) forms of A3G were detected in redoxal-treated cells and virions produced from these cells (Fig. 3C). These HMW forms might

represent Vif-induced polyubiquitinated A3G; in that case, the decrease in cellular Vif protein levels detected at 6 days compared to 3 days post-infection might explain the lack of HMW forms of A3G detected at day 6. Redoxal treatment also increased A3G incorporation into virions based on analysis of A3G in virions produced from CEM cells and quantification of virion-associated A3G and p24^{Gag} and the ratio of A3G: p24^{Gag} proteins.

Redoxal attenuation of viral infectivity is augmented in cells expressing A3G

To further characterize redoxal attenuation of HIV-1 replication in T cells, we tested whether redoxal treatment enhances A3G antiviral activity in a single-round infectivity assay. VSV-G pseudotyped NL4-3GFP Env viruses were produced in the presence of A3G in redoxal-treated 293T producer cells. Similar to what we observed in redoxal-treated CEM T cells, A3G protein levels were elevated and Vif expression was suppressed in redoxal-treated 293T cells (Fig. 4A). Quantification of HIV-1 particles produced from these cells by RT assay demonstrated that redoxal treatment also inhibited virus production (Fig. 4B). Equivalent amounts of virus were used to infect TZM-bl reporter cells, which showed that virions produced in redoxal-treated cells were less infectious than virus particles produced in untreated cells (Fig. 4C). Redoxal treatment reduced virus production and virion infectivity regardless of A3G expression (Fig. 4C). Redoxal inhibited HIV-1 infectivity by approximately 20% in the absence of A3G and approximately 40% in the presence of A3G. These results, together with those of Fig. 3A and other experiments suggest that about half of its antiviral activity is achieved through A3G-dependent activity, while the other half of its antiviral activity is A3G-independent.

Redoxal increases A3G protein stability in cells expressing HIV-1 Vif

Based on its identification in a high-throughput screen designed to identify inhibitors of Vif-A3G binding, we expected that redoxal treatment would directly disrupt the Vif-A3G protein-protein interaction and hypothesized that this liberation of A3G from Vif binding would directly lead to A3G stabilization. To examine this possibility, 293T cells were co-transfected with Vif-FLAG and A3G-HA plasmids and treated with 1250 nM redoxal for 40 h. As seen in the preceding experiments (Fig. 4A), redoxal treatment abolished Vif-dependent A3G degradation (Fig. 5B, upper panel). To test whether the increase in A3G protein could be attributed to increased stability of the A3G protein, cycloheximide (CHX) was used to arrest protein translation in cells and the effects of redoxal treatment on A3G protein levels were monitored over a 4-hour time course. 293T cells were co-transfected with A3G-3xHA and pNL4-3GFP Env plasmids and treated with 1250 nM redoxal for 36 h, followed by CHX treatment. Cells were harvested at different time points and A3G and HIV-1 Vif protein levels were examined in cell lysates by Western blotting followed by quantitative analysis of protein levels using densitometry (Fig. 5A). The CHX time course showed that steady-state levels of A3G protein were stabilized by redoxal treatment, while in the absence of redoxal A3G levels were decreased by approximately 50%. In contrast, redoxal had no significant effect on Vif protein stability (Fig. 5A).

Redoxal does not affect Vif interaction with A3G or Cullin 5 in cells

Contrary to expectations, co-immunoprecipitation of Vif and A3G proteins from lysates of redoxal-treated versus untreated cells did not reveal any significant effect of redoxal

treatment on Vif-A3G interaction in cells (Fig. 5B, lower panel). However, the experimental conditions of the co-immunoprecipitation assay are markedly different from those of the TR-FRET assay, which could affect the ability to detect Vif-A3G interaction. Because Vif-A3G interaction did not appear to be affected by redoxal treatment yet A3G was still liberated from Vif-mediated degradation, we next determined whether redoxal was potentially affecting the ability of Vif to interact with Cul5. Co-immunoprecipitation of HA-Cul5 from 293T cells expressing Vif-FLAG and HA-Cul5 indicated that redoxal treatment has no effect on Vif-Cul5 interaction (Fig. 5C). These results, together with the preceding experiments, suggest that redoxal has no major effect on the interaction of Vif with A3G or Cul5 proteins.

Redoxal exerts its effects on A3G antiviral activity through pyrimidine depletion

Redoxal inhibits *de novo* pyrimidine synthesis by inhibiting DHODH, the fourth enzyme of this pathway that converts dihydroorotate to orotate. Recent studies showed that other inhibitors of pyrimidine biosynthesis are potent broad-spectrum antivirals (Hoffmann et al., 2011; Lucas-Hourani et al., 2013). Therefore, we explored the role of pyrimidine availability in regulation of A3G protein levels in cells and virions by examining the effects of supplementation with uridine, which serves a central role in salvage pathways for pyrimidine synthesis, and orotate, a pyrimidine precursor. NL4-3GFP Env viruses were produced in A3G-expressing 293T cells treated with redoxal and supplemented with uridine or orotate. A3G protein levels in cells and virions were compared to those of untreated controls by Western blotting followed by quantitative analysis of A3G protein levels using densitometry. Consistent with preceding experiments (Fig. 5), redoxal treatment increased A3G protein levels in virus producer cells expressing HIV-1 Vif by approximately 50% (Fig. 6A and B). If the effects of redoxal on A3G protein levels were related to its ability to inhibit pyrimidine synthesis, we would expect to find that supplementation with uridine or orotate would reverse the effects of redoxal treatment. Supporting this hypothesis, the effects of redoxal treatment on A3G protein levels were reversed by supplementation with uridine (50 μM) or orotate (2 mM), while Vif and p55^{Gag} levels were not affected (Fig. 6A, upper panel, and 6B). Furthermore, the increase in encapsidated A3G protein in virions produced from redoxal-treated cells was reversed by treatment with 50 μM uridine (Fig. 6A, lower panel). A3G has been detected in exosomes, which have similar size and density as HIV-1 virions; the results shown in Fig. 6A (lower panel) may therefore represent A3G proteins in both HIV-1 virions and secreted exosomes (Coren et al., 2008; Khatua et al., 2009). Consistent with these findings, an approximately 50% decrease in the infectivity of NL4-3GFP Env viruses produced in redoxal-treated 293T producer cells was reversed by treatment with 50 μM uridine or 2 mM orotate (Fig. 6C and D). The moderate effect of 2 mM orotate compared to 50 uM uridine on diminishing redoxal antiviral activity is consistent with another study (Lucas-Hourani et al., 2013). These results suggest that redoxal augments A3G protein levels and antiviral activity through its ability to inhibit pyrimidine synthesis.

To determine if redoxal treatment and uridine or orotate supplementation have similar effects on A3G protein levels in cells in the absence of Vif expression, we performed subsequent experiments in 293T cells expressing A3G but not Vif or other viral proteins.

These experiments showed that A3G protein levels were increased by redoxal treatment, while exposure to 50 μM uridine or 2 mM orotate reversed this effect of redoxal (Fig. 7A and B). In the absence of redoxal treatment, uridine or orotate treatment had no significant effect on A3G protein levels. Finally, we examined whether pyrimidine depletion by redoxal treatment affected cell viability. Treatment with redoxal (1250 nM) led to a 35% decrease in cell viability, while orotate supplementation reversed this effect in a dose-dependent manner, suggesting that pyrimidine depletion by redoxal decreases cell viability (Fig. 7C).

Pyrimidine depletion by redoxal augments A3G protein stability

To assess whether pyrimidine depletion by redoxal increases A3G protein stability in the presence or absence of Vif, 293T cells were co-transfected with A3G-3xHA and pNL4-3GFP Env (Fig. 8A) or pCDNA3.1 (Fig. 8B) plasmids and treated for 36 h with or without redoxal and uridine supplementation followed by CHX treatment. At 0 or 4 h CHX treatment, cells were harvested to examine A3G and HIV-1 Vif protein levels by Western blotting. In the presence (Fig. 8A) or absence of HIV-1 Vif (Fig. 8B), CHX treatment had no significant effect on A3G protein levels in cells treated with redoxal alone or supplemented with uridine, suggesting that pyrimidine depletion induced by redoxal increases A3G protein stability through a Vif-independent mechanism. In the absence of Vif (Fig. 8B), redoxal appears to increase A3G more than in the presence of Vif (Fig. 6A and 8A), which may be due to differences in the experimental conditions, shorter exposure time of the blot in Fig. 8B, and/or effects of redoxal on Vif-mediated A3G degradation.

DISCUSSION

In this study, we report the initial characterization of two compounds identified in a high-throughput screen for inhibitors of Vif-A3G interaction (Fig. 1A). Both compounds potently suppressed HIV-1 replication in PBMCs and human T cell lines. Lomofungin is a natural product originally isolated from bacteria. While the specific cellular targets of lomofungin have not been identified, its inhibition of RNA synthesis is well characterized (Cano et al., 1973; Johnson and Dietz, 1969; Klo et al., 1973) and it has also been shown to inhibit the botulinum neurotoxin light chain protease (Eubanks et al., 2010) and was identified as a potential therapeutic for myotonic dystrophy type 1 (Hoskins et al., 2014b). However, its therapeutic potential is limited by cytotoxicity, demonstrated in the present study as well as prior studies. In an attempt to identify non-cytotoxic analogs, we performed structure-activity relationship (SAR) studies (Additional Files 2 and 3). We identified one lomofungin analog (analog 4) that exhibited antiviral activity against several HIV-1 isolates and minimal cytotoxicity. However, this analog exerted only weak antiviral activity. Therefore, further structural optimization is needed to identify optimized compounds that may have stronger antiviral activity and better therapeutic index.

Redoxal, the more potent compound identified in the present study, demonstrated broad antiviral activity, inhibiting replication of diverse HIV-1 isolates in PBMCs and T cell lines. Redoxal is a known inhibitor of *de novo* pyrimidine synthesis (Cleaveland et al., 1995; Zameitat et al., 2006) and redoxal treatment leads to pyrimidine depletion in cells (Knecht and Loffler, 2000). Previously, the antiviral effects of pyrimidine on nucleotide depletion

centered on decreased free nucleoside pools and potential interference with viral synthesis of nucleic acids. However, in the last several years, several groups have identified diverse molecules that inhibit pyrimidine biosynthesis and suppress viral growth (A3 and DD264), with cellular profiles suggesting mechanisms of antiviral resistance induction that extend beyond limitation of free nucleosides (Hoffmann et al., 2011; Lucas-Hourani et al., 2013). The antiviral activity of pyrimidine biosynthesis inhibitors such as A3 and DD264 has been demonstrated mainly against RNA viruses (e.g., influenza viruses A and B, Sendai virus, vesicular stomatitis virus, hepatitis C virus, West Nile virus and Dengue I virus), although some activity against DNA viruses (e.g., adenovirus 5, vaccinia, and a polyomavirus) has also been shown (DeVito et al., 2014; Hoffmann et al., 2011; Lucas-Hourani et al., 2013). Consistent with findings in the present study, earlier studies showed that the pyrimidine synthesis inhibitors leflunomide (used clinically as an immunosuppressive anti-rheumatic drug) and A3 have antiviral activity against HIV-1 (Hoffmann et al., 2011; Schlapfer et al., 2003). Recent work has expanded our understanding of mechanisms through which these pyrimidine synthesis inhibitors lead to viral restriction. Based on recent studies, it has become increasingly clear that intracellular skewing of nucleoside pools leads to a generalized antiviral state adopted by cells (Lucas-Hourani et al., 2013). This antiviral state is mediated, at least in part, through induction of well-characterized innate immunity signaling networks that culminate in increased expression of intracellular defense genes mapping to the type I interferon response pathway. Sensitization to apoptosis may occur in parallel (Setzer et al., 2008), an effect that may contribute to the cytotoxic effects we observed in redoxal-treated cells.

Redoxal exhibited stronger antiviral activity in the presence of A3G expression, suggesting involvement of an A3G-dependent mechanism and consistent with identification of redoxal in a high throughput screen targeting Vif-A3G interaction. However, we also found that about half of its antiviral activity was A3G-independent, suggesting that protective effects of redoxal are likely to be pleiotropic. Redoxal's A3G-independent activity may target the virus at a post-integration step(s) prior to virion maturation, such as the step of transcription, similar to the pyrimidine synthesis inhibitor A3 (Hoffmann et al., 2011). Exploring its molecular mechanism of action revealed an unexpected stabilization of A3G protein in redoxal-treated cells. Contrary to expectations, specific disruption of the Vif-A3G interaction was not detected, although Vif protein levels appeared to be moderately suppressed while A3G protein levels were increased. Importantly, pyrimidine depletion induced by redoxal not only increased cellular A3G protein levels; its anti-HIV-1 activity was also enhanced. To our knowledge, this is the first report to identify a direct link between induction of a generalized antiviral state via inhibition of pyrimidine biosynthesis and a specific cellular restriction factor.

The antiviral mechanisms induced by redoxal have not been characterized in detail, nor have the direct intracellular targets been identified. Redoxal-mediated restriction of HIV-1 appears to affect late steps in the viral replication cycle, consistent with previous studies of the pyrimidine synthesis inhibitor A3 (Hoffmann et al., 2011). In unpublished preliminary experiments, redoxal did not disrupt Vif-CBFβ interaction in co-immunoprecipitation experiments similar to those shown in Fig. 5. However, further studies are needed to determine if CBFβ has any role in redoxal's antiviral activity. Redoxal treatment may also

impair protein degradation (Tolstonog and Deppert, 2010). In the presence of redoxal, we detected high molecular weight forms of A3G that might represent mono- and polyubiquitinated A3G proteins, potentially rescued from proteasomal degradation and accumulating in infected cells and newly produced viruses. The possibility that these alternate forms of A3G represent ubiquitinated proteins and their functional significance will be addressed in future studies. Most intriguing is the newly identified link between disruption of the intracellular nucleoside availability and initiation of a potent innate antiviral response through A3G-dependent as well as A3G-independent mechanisms. It is interesting to consider whether cellular pyrimidine depletion by redoxal treatment of A3G-expressing T cells initiates an antiviral program through induction of an as yet unidentified pathway that culminates in augmentation of A3G, a potent restriction factor mediating innate immunity, leading to enhanced restriction against an invading retrovirus. For example, pyrimidine depletion may induce mismatch repair, leading to a DNA damage response and activation of DNA-damage-induced signaling pathways that could be involved in regulating A3G stability (Franchini and Petersen-Mahrt, 2014).

In summary, we identified lomofungin and redoxal as novel inhibitors of HIV-1 replication. Studies exploring the mechanisms mediating redoxal antiviral activity suggest that inhibition of pyrimidine biosynthesis and limited pyrimidine availability increase cellular A3G protein stability and antiviral activity, thereby restricting HIV-1 infection. A better understanding of the connections between dysregulation of cellular nucleoside pools and induction of the innate restriction factor A3G may provide insights that will be helpful for future development of novel antiviral strategies.

METHODS

Cells

HEK293T cells (ATCC) were grown in DMEM supplemented with 10% fetal bovine serum and 1% penicillin/streptomycin. TZM-bl cells (obtained through the NIH AIDS Reagent Program, Division of AIDS, NIAID, NIH: TZM-bl from Dr. John C. Kappes, Dr. Xiaoyun Wu and Tranzyme Inc.(Wei et al., 2002)) were grown in DMEM supplemented with 10% FBS and 1% penicillin/streptomycin. The T cell lines H9, CEM, CEM-SS, and SupT1 (obtained through the NIH AIDS Reagent Program) were grown in RPMI 1640 supplemented with 10% FBS and 1% penicillin/streptomycin. Fresh human PBMCs were isolated as previously described (Ptak et al., 2008) from screened donors, seronegative for HIV and HBV (Biological Specialty Corporation, Colmar, PA) and grown in RPMI 1640 supplemented with 15% FBS, 2 mM L-glutamine, 100 U/mL penicillin, and 100 μg/mL streptomycin; cells were stimulated with 4 μg/mL phytohemagglutinin (PHA; Sigma-Aldrich) for 48–72 h and cultured in RPMI 1640 supplemented with 15% FBS, L-glutamine, penicillin, streptomycin, non-essential amino acids (MEM/NEAA; Hyclone) and 20 U/mL recombinant human IL-2 (R&D Systems Inc.) for 48 h before infection.

Antibodies and Plasmids

The following antibodies were used: rabbit anti-Vif (Goncalves et al., 1994), rat 3F10 anti-HA (Roche Applied Science), mouse anti-tubulin (Sigma-Aldrich), mouse anti-GFP

(Zymed), and rabbit anti-APOBEC3G (obtained through the NIH AIDS Reagent Program, Division of AIDS, NIAID, NIH: anti-APOBEC3G-C terminal from Dr. Jaisri Lingappa). pNL4-3-GFP is pNL4-3, an HIV-1 proviral DNA containing plasmid, with an *env*-inactivating mutation and enhanced green fluorescent protein (eGFP) replacing *nef* (He et al., 1997). pNLA1.Vif-FLAG was a gift from K. Strebel (Strebel, 2013). pCMV4.APOBEC3G-HA was a gift from M. Malim (Sheehy et al., 2002). pCDNA3-HA-Cul5 was a gift from J. Conaway. The pGEX.6P.1 expression vector (Novagen) expresses Vif residues 1–94.

Cell transfection, Western Blot Analysis, and Co-immunoprecipitation

HEK293T cells were cultured in DMEM with 10% FBS and transfected by lipofectamine 2000 (Life Technologies) according to the manufacturer's instructions. 40–48 h post transfection, cells were lysed in lysis buffer (50 mM Tris-HCl, pH 7.0, 150 mM NaCl, 0.5% Nonidet P-40, and 1% protease inhibitor mixture). Twenty-five μg of protein normalized by Bradford protein assay (Bio-Rad) was separated by SDS-PAGE, transferred onto polyvinylidene difluoride (PVDF) membranes (Millipore), and detected by standard Western blotting. For co-immunoprecipitation experiments, identical amounts of lysate were subjected to immunoprecipitation followed by Western blotting. HA- and FLAG-tagged proteins were immunoprecipitated by EZview Red Anti-HA Affinity Gel (Sigma-Aldrich) and FLAG-Immunopecipitation Kit (Sigma-Aldrich).

High-throughput Screen for Inhibitors of Vif-APOBEC3G Interaction

The homogeneous time-resolved fluorescence energy transfer (TR-FRET) assay for inhibitors of Vif-A3G interaction was previously described (Pery et al., 2015). Briefly, the interaction between GST-Vif residues 1–94, which contains the A3G binding site, and a biotinylated peptide consisting of A3G residues 110–148 was detected using TR-FRET (Mehle et al., 2007; Pery et al., 2009). The 1–94 GST-Vif was expressed and purified from *E.coli* as described (Pery et al., 2009). A 307,520 compound library (NIH Molecular Libraries Small Molecule Repository (MLSMR)) was screened at 6.25 μM and hits were selected based on percent inhibition of 1–94 GST-Vif and A3G peptide interaction as described (Pery et al., 2015). Candidates were further evaluated for dose-response (ranging between 0.195 and 100 μM) in a counter screen to exclude compounds attenuating the TR-FRET signal independently of Vif-A3G interaction, and in an HIV-1 Tat-TAR Fluorescence Polarization (FP) assay to aid in selecting compounds with specificity for the Vif-A3G interaction. Candidates were also evaluated in a cell toxicity assay. Detailed methods of the counter screens and cytotoxicity screens have been described (Pery et al., 2015).

HIV-1 Replication in Peripheral Blood Mononuclear Cells

Compounds were evaluated in dose-response assays using a 100 μM high-test concentration as described (Ptak et al., 2008). AZT was included as a positive control. Activated PBMCs were plated at 50×10^4 cells/well in 96-well plates. An MOI of ~0.1 of HIV-1$_{Ba-L}$ (lab-adapted, Group M, Subtype B, CCR5-tropic; from the NIH AIDS Reagent Program, Division of AIDS, NIAID, NIH, courtesy of Drs. Suzanne Gartner, Mikulas Popovic, and Robert Gallo (Gartner et al., 1986)), or one of the following HIV-1 isolates from the NIH

AIDS Reagent Program: HIV-1$_{NL4-3}$ (lab-adapted, Group M, Subtype B, CXCR4-tropic; from Dr. Malcolm Martin), HIV-1 89BZ167 (clinical isolate, Group M, Subtype B, CXCR4-tropic; from the NIH AIDS Reagent Program, Division of AIDS, NIAID, NIH, courtesy of Dr. John Mascola (Louwagie et al., 1994)), or HIV-1 91US001 (alternative designations US1 (GS 004) or 91US_1; clinical isolate, Group M, Subtype B, CCR5-tropic from the NIH AIDS Reagent Program, Division of AIDS, NIAID, NIH, courtesy of Dr. Nelson Michael (Jagodzinski et al., 2000; Michael et al., 1999; Vahey et al., 1999)) was then added to each test well. Primary virus stocks were prepared by low-passage replication in fresh PBMCs. Parallel plates without virus were prepared and monitored for cell viability using MTS (CellTiter 96 Reagent, Promega). PBMC cultures were maintained for 7 days at 37°C, 5% CO_2. Cell-free supernatants were then collected and analyzed for reverse transcriptase (RT) activity (Buckheit and Swanstrom, 1991), while cytotoxicity was measured by MTS assay.

HIV-1 Replication in T cells

NL4-3 (X4-tropic) viruses were produced in HEK293T cells and viral titers were measured by RT assay as described (Goncalves et al., 1996). Virus stocks of 1×10^5 ^{3}H cpm and 2×10^4 ^{3}H cpm were used to infect 10^6 H9 or SupT1 T cells, respectively. 3 h post incubation at 37°C, 5% CO_2, infected cells were washed 3x to remove cell-free virus and 100 μL of infected cells were added to wells in 96-well plates. Lomofungin (Enzo Life Sciences) was evaluated in dose-response assays using a 250 nM high-test concentration. The protease inhibitor Ritonavir was included as a positive control (obtained through the NIH AIDS Reagent Program). Plates without virus were prepared in parallel for cytotoxicity assays. Cells were incubated for 6 days, and virus production was measured using p24 ELISA (PerkinElmer) according to the manufacturer's instructions; cytotoxicity was measured by CellTiter-Glo® assay. Redoxal (Sigma Aldrich) was evaluated for antiviral activity during spreading infections in CEM and CEM-SS T cells infected with HIV-1$_{NL4-3}$. At 3 h post-infection, cells were treated with increasing concentrations of redoxal and virus production and viability of treated cells was tested at 3, 6, and 9 days post-infection by RT and CellTiter-Glo® assays.

Viral Infectivity Assay and Virus Purification

Viruses were produced by co-transfecting HEK293T cells with VSV-G envelope glycorprotein, pCMV4.APOBEC3G-HA, and pNL4-3GFP Env HIV-1 plasmids (He et al., 1997). Viruses were quantified by RT assays, and normalized amounts were used to infect the reporter cell line TZM-bl. Infectivity was measured 48 h after infection by performing luciferase (Promega) or β-galactosidase assays (Applied Biosystems). To purify viruses, 1.5×10^5 cpm virus-containing supernatants were concentrated by ultracentrifugation through 20% sucrose in phosphate-buffered saline (PBS). Purified viruses were resuspended in Laemmli sample buffer supplemented with 5% β-mercaptoethanol. p24Gag and A3G protein levels in purified virus particles were detected by Western blot.

Statistical Analysis

Statistical significance was determined using Student's unpaired 2-tailed *t*-test, with results presented as means of duplicate or triplicate independent wells or samples. Error bars represent standard deviations. P-values < 0.05 were considered significant.

Supplementary Material

Refer to Web version on PubMed Central for supplementary material.

Acknowledgments

References

Aires da Silva F, Santa-Marta M, Freitas-Vieira A, Mascarenhas P, Barahona I, Moniz-Pereira J, Gabuzda D, Goncalves J. Camelized rabbit-derived VH single-domain intrabodies against Vif strongly neutralize HIV-1 infectivity. Journal of molecular biology. 2004; 340:525–542. [PubMed: 15210352]

Belanger K, Savoie M, Rosales Gerpe MC, Couture JF, Langlois MA. Binding of RNA by APOBEC3G controls deamination-independent restriction of retroviruses. Nucleic acids research. 2013; 41:7438–7452. [PubMed: 23761443]

Bishop KN, Holmes RK, Malim MH. Antiviral potency of APOBEC proteins does not correlate with cytidine deamination. Journal of virology. 2006; 80:8450–8458. [PubMed: 16912295]

Bogerd HP, Doehle BP, Wiegand HL, Cullen BR. A single amino acid difference in the host APOBEC3G protein controls the primate species specificity of HIV type 1 virion infectivity factor. Proceedings of the National Academy of Sciences of the United States of America. 2004; 101:3770–3774. [PubMed: 14999100]

Bonavia A, Franti M, Pusateri Keaney E, Kuhen K, Seepersaud M, Radetich B, Shao J, Honda A, Dewhurst J, Balabanis K, Monroe J, Wolff K, Osborne C, Lanieri L, Hoffmaster K, Amin J, Markovits J, Broome M, Skuba E, Cornella-Taracido I, Joberty G, Bouwmeester T, Hamann L, Tallarico JA, Tommasi R, Compton T, Bushell SM. Identification of broad-spectrum antiviral compounds and assessment of the druggability of their target for efficacy against respiratory syncytial virus (RSV). Proceedings of the National Academy of Sciences of the United States of America. 2011; 108:6739–6744. [PubMed: 21502533]

Buckheit RW Jr, Swanstrom R. Characterization of an HIV-1 isolate displaying an apparent absence of virion-associated reverse transcriptase activity. AIDS research and human retroviruses. 1991; 7:295–302. [PubMed: 1712216]

Cano FR, Kuo SC, Lampen JO. Lomofungin, an inhibitor of deoxyribonucleic acid-dependent ribonucleic acid polymerases. Antimicrobial agents and chemotherapy. 1973; 3:723–728. [PubMed: 4790624]

Carr A, Cooper DA. Adverse effects of antiretroviral therapy. Lancet. 2000; 356:1423–1430. [PubMed: 11052597]

Cen S, Peng ZG, Li XY, Li ZR, Ma J, Wang YM, Fan B, You XF, Wang YP, Liu F, Shao RG, Zhao LX, Yu L, Jiang JD. Small molecular compounds inhibit HIV-1 replication through specifically stabilizing APOBEC3G. The Journal of biological chemistry. 2010; 285:16546–16552. [PubMed: 20363737]

Chaurasiya KR, McCauley MJ, Wang W, Qualley DF, Wu T, Kitamura S, Geertsema H, Chan DS, Hertz A, Iwatani Y, Levin JG, Musier-Forsyth K, Rouzina I, Williams MC. Oligomerization transforms human APOBEC3G from an efficient enzyme to a slowly dissociating nucleic acid-binding protein. Nature chemistry. 2014; 6:28–33.

Chung DH, Jonsson CB, Maddox C, McKellip SN, Moore BP, Heil M, White EL, Ananthan S, Li Q, Feng S, Rasmussen L. HTS-driven discovery of new chemotypes with West Nile Virus inhibitory activity. Molecules. 2010; 15:1690–1704. [PubMed: 20336008]

Cleaveland ES, Monks A, Vaigro-Wolff A, Zaharevitz DW, Paull K, Ardalan K, Cooney DA, Ford H Jr. Site of action of two novel pyrimidine biosynthesis inhibitors accurately predicted by the compare program. Biochemical pharmacology. 1995; 49:947–954. [PubMed: 7741767]

Coren LV, Shatzer T, Ott DE. CD45 immunoaffinity depletion of vesicles from Jurkat T cells demonstrates that exosomes contain CD45: no evidence for a distinct exosome/HIV-1 budding pathway. Retrovirology. 2008; 5:64. [PubMed: 18631400]

Dang Y, Davis RW, York IA, Zheng YH. Identification of 81LGxGxxIxW89 and 171EDRW174 domains from human immunodeficiency virus type 1 Vif that regulate APOBEC3G and APOBEC3F neutralizing activity. Journal of virology. 2010a; 84:5741–5750. [PubMed: 20335268]

Dang Y, Wang X, York IA, Zheng YH. Identification of a critical T(Q/D/E)x5ADx2(I/L) motif from primate lentivirus Vif proteins that regulate APOBEC3G and APOBEC3F neutralizing activity. Journal of virology. 2010b; 84:8561–8570. [PubMed: 20592083]

DeVito SR, Ortiz-Riano E, Martinez-Sobrido L, Munger J. Cytomegalovirus-mediated activation of pyrimidine biosynthesis drives UDP-sugar synthesis to support viral protein glycosylation. Proceedings of the National Academy of Sciences of the United States of America. 2014; 111:18019–18024. [PubMed: 25472841]

Esnault C, Heidmann O, Delebecque F, Dewannieux M, Ribet D, Hance AJ, Heidmann T, Schwartz O. APOBEC3G cytidine deaminase inhibits retrotransposition of endogenous retroviruses. Nature. 2005; 433:430–433. [PubMed: 15674295]

Esnault C, Millet J, Schwartz O, Heidmann T. Dual inhibitory effects of APOBEC family proteins on retrotransposition of mammalian endogenous retroviruses. Nucleic acids research. 2006; 34:1522–1531. [PubMed: 16537839]

Eubanks LM, Silhar P, Salzameda NT, Zakhari JS, Xiaochuan F, Barbieri JT, Shoemaker CB, Hixon MS, Janda KD. Identification of a Natural Product Antagonist against the Botulinum Neurotoxin Light Chain Protease. ACS medicinal chemistry letters. 2010; 1:268–272. [PubMed: 20959871]

Franchini DM, Petersen-Mahrt SK. AID and APOBEC deaminases: balancing DNA damage in epigenetics and immunity. Epigenomics. 2014; 6:427–443. [PubMed: 25333851]

Gartner S, Markovits P, Markovitz DM, Kaplan MH, Gallo RC, Popovic M. The role of mononuclear phagocytes in HTLV-III/LAV infection. Science. 1986; 233:215–219. [PubMed: 3014648]

Gillick K, Pollpeter D, Phalora P, Kim EY, Wolinsky SM, Malim MH. Suppression of HIV-1 infection by APOBEC3 proteins in primary human CD4(+) T cells is associated with inhibition of processive reverse transcription as well as excessive cytidine deamination. Journal of virology. 2013; 87:1508–1517. [PubMed: 23152537]

Goila-Gaur R, Strebel K. HIV-1 Vif, APOBEC, and intrinsic immunity. Retrovirology. 2008; 5:51. [PubMed: 18577210]

Goncalves J, Jallepalli P, Gabuzda DH. Subcellular localization of the Vif protein of human immunodeficiency virus type 1. Journal of virology. 1994; 68:704–712. [PubMed: 8289374]

Goncalves J, Korin Y, Zack J, Gabuzda D. Role of Vif in human immunodeficiency virus type 1 reverse transcription. Journal of virology. 1996; 70:8701–8709. [PubMed: 8970997]

Goncalves J, Silva F, Freitas-Vieira A, Santa-Marta M, Malho R, Yang X, Gabuzda D, Barbas C 3rd. Functional neutralization of HIV-1 Vif protein by intracellular immunization inhibits reverse transcription and viral replication. The Journal of biological chemistry. 2002; 277:32036–32045. [PubMed: 12039955]

Guo F, Cen S, Niu M, Yang Y, Gorelick RJ, Kleiman L. The interaction of APOBEC3G with human immunodeficiency virus type 1 nucleocapsid inhibits tRNA3Lys annealing to viral RNA. Journal of virology. 2007; 81:11322–11331. [PubMed: 17670826]

Guo Y, Dong L, Qiu X, Wang Y, Zhang B, Liu H, Yu Y, Zang Y, Yang M, Huang Z. Structural basis for hijacking CBF-beta and CUL5 E3 ligase complex by HIV-1 Vif. Nature. 2014; 505:229–233. [PubMed: 24402281]

Harris RS, Bishop KN, Sheehy AM, Craig HM, Petersen-Mahrt SK, Watt IN, Neuberger MS, Malim MH. DNA deamination mediates innate immunity to retroviral infection. Cell. 2003; 113:803–809. [PubMed: 12809610]

He J, Chen Y, Farzan M, Choe H, Ohagen A, Gartner S, Busciglio J, Yang X, Hofmann W, Newman W, Mackay CR, Sodroski J, Gabuzda D. CCR3 and CCR5 are co-receptors for HIV-1 infection of microglia. Nature. 1997; 385:645–649. [PubMed: 9024664]

Hoffmann HH, Kunz A, Simon VA, Palese P, Shaw ML. Broad-spectrum antiviral that interferes with de novo pyrimidine biosynthesis. Proceedings of the National Academy of Sciences of the United States of America. 2011; 108:5777–5782. [PubMed: 21436031]

Holmes RK, Malim MH, Bishop KN. APOBEC-mediated viral restriction: not simply editing? Trends Biochem Sci. 2007; 32:118–128. [PubMed: 17303427]

Hoskins JW, Ofori LO, Chen CZ, Kumar A, Sobczak K, Nakamori M, Southall N, Patnaik S, Marugan JJ, Zheng W, Austin CP, Disney MD, Miller BL, Thornton CA. Lomofungin and dilomofungin: inhibitors of MBNL1-CUG RNA binding with distinct cellular effects. Nucleic acids research. 2014a; 42:6591–6602. [PubMed: 24799433]

Hoskins JW, Ofori LO, Chen CZ, Kumar A, Sobczak K, Nakamori M, Southall N, Patnaik S, Marugan JJ, Zheng W, Austin CP, Disney MD, Miller BL, Thornton CA. Lomofungin and dilomofungin: inhibitors of MBNL1-CUG RNA binding with distinct cellular effects. Nucleic Acids Res. 2014b

Huthoff H, Malim MH. Identification of amino acid residues in APOBEC3G required for regulation by human immunodeficiency virus type 1 Vif and Virion encapsidation. Journal of virology. 2007; 81:3807–3815. [PubMed: 17267497]

Jager S, Kim DY, Hultquist JF, Shindo K, LaRue RS, Kwon E, Li M, Anderson BD, Yen L, Stanley D, Mahon C, Kane J, Franks-Skiba K, Cimermancic P, Burlingame A, Sali A, Craik CS, Harris RS, Gross JD, Krogan NJ. Vif hijacks CBF-beta to degrade APOBEC3G and promote HIV-1 infection. Nature. 2012; 481:371–375. [PubMed: 22190037]

Jagodzinski LL, Wiggins DL, McManis JL, Emery S, Overbaugh J, Robb M, Bodrug S, Michael NL. Use of calibrated viral load standards for group M subtypes of human immunodeficiency virus type 1 to assess the performance of viral RNA quantitation tests. Journal of clinical microbiology. 2000; 38:1247–1249. [PubMed: 10699033]

Johnson LE, Dietz A. Lomofungin, a new antibiotic produced by Streptomyces lomondensis sp. n. Applied microbiology. 1969; 17:755–759. [PubMed: 5785961]

Kalayjian RC, Lau B, Mechekano RN, Crane HM, Rodriguez B, Salata RA, Krishnasami Z, Willig JH, Martin JN, Moore RD, Eron JJ, Kitahata MM. Risk factors for chronic kidney disease in a large cohort of HIV-1 infected individuals initiating antiretroviral therapy in routine care. Aids. 2012; 26:1907–1915. [PubMed: 22824630]

Kao S, Khan MA, Miyagi E, Plishka R, Buckler-White A, Strebel K. The human immunodeficiency virus type 1 Vif protein reduces intracellular expression and inhibits packaging of APOBEC3G (CEM15), a cellular inhibitor of virus infectivity. Journal of virology. 2003; 77:11398–11407. [PubMed: 14557625]

Kao S, Miyagi E, Khan MA, Takeuchi H, Opi S, Goila-Gaur R, Strebel K. Production of infectious human immunodeficiency virus type 1 does not require depletion of APOBEC3G from virus-producing cells. Retrovirology. 2004; 1:27. [PubMed: 15373943]

Ketseoglou I, Lukhwareni A, Steegen K, Carmona S, Stevens WS, Papathanasopoulos MA. Viral tropism and antiretroviral drug resistance in HIV-1 subtype C-infected patients failing highly

active antiretroviral therapy in Johannesburg, South Africa. AIDS research and human retroviruses. 2014; 30:289–293. [PubMed: 24224886]

Khatua AK, Taylor HE, Hildreth JE, Popik W. Exosomes packaging APOBEC3G confer human immunodeficiency virus resistance to recipient cells. Journal of virology. 2009; 83:512–521. [PubMed: 18987139]

Klo SC, Cano FR, Lampen JO. Lomofungin, an inhibitor of ribonucleic acid synthesis in yeast protoplasts: its effect on enzyme formation. Antimicrobial agents and chemotherapy. 1973; 3:716–722. [PubMed: 4790623]

Knecht W, Loffler M. Redoxal as a new lead structure for dihydroorotate dehydrogenase inhibitors: a kinetic study of the inhibition mechanism. FEBS letters. 2000; 467:27–30. [PubMed: 10664450]

Kouno T, Luengas EM, Shigematsu M, Shandilya SM, Zhang J, Chen L, Hara M, Schiffer CA, Harris RS, Matsuo H. Structure of the Vif-binding domain of the antiviral enzyme APOBEC3G. Nature structural & molecular biology. 2015; 22:485–491.

Kumar M, Sen S, Gupta RK, Chaturbhuj D, Tripathy SP, Paranjape RS. Prevalence of drug resistance in human immunodeficiency virus type 1-infected treatment-naive children in Pune, India. AIDS research and human retroviruses. 2014; 30:294–298. [PubMed: 24387706]

Li JZ, Gallien S, Do TD, Martin JN, Deeks S, Kuritzkes DR, Hatano H. Prevalence and significance of HIV-1 drug resistance mutations among patients on antiretroviral therapy with detectable low-level viremia. Antimicrobial agents and chemotherapy. 2012; 56:5998–6000. [PubMed: 22890763]

Louwagie J, Delwart EL, Mullins JI, McCutchan FE, Eddy G, Burke DS. Genetic analysis of HIV-1 isolates from Brazil reveals presence of two distinct genetic subtypes. AIDS research and human retroviruses. 1994; 10:561–567. [PubMed: 7917518]

Lucas-Hourani M, Dauzonne D, Jorda P, Cousin G, Lupan A, Helynck O, Caignard G, Janvier G, Andre-Leroux G, Khiar S, Escriou N, Despres P, Jacob Y, Munier-Lehmann H, Tangy F, Vidalain PO. Inhibition of pyrimidine biosynthesis pathway suppresses viral growth through innate immunity. PLoS pathogens. 2013; 9:e1003678. [PubMed: 24098125]

Luo K, Wang T, Liu B, Tian C, Xiao Z, Kappes J, Yu XF. Cytidine deaminases APOBEC3G and APOBEC3F interact with human immunodeficiency virus type 1 integrase and inhibit proviral DNA formation. Journal of virology. 2007; 81:7238–7248. [PubMed: 17428847]

Malim MH. APOBEC proteins and intrinsic resistance to HIV-1 infection. Philosophical transactions of the Royal Society of London. Series B, Biological sciences. 2009; 364:675–687.

Malim MH, Bieniasz PD. HIV Restriction Factors and Mechanisms of Evasion. Cold Spring Harbor perspectives in medicine. 2012; 2:a006940. [PubMed: 22553496]

Mangeat B, Turelli P, Caron G, Friedli M, Perrin L, Trono D. Broad antiretroviral defence by human APOBEC3G through lethal editing of nascent reverse transcripts. Nature. 2003; 424:99–103. [PubMed: 12808466]

Mangeat B, Turelli P, Liao S, Trono D. A single amino acid determinant governs the species-specific sensitivity of APOBEC3G to Vif action. The Journal of biological chemistry. 2004; 279:14481–14483. [PubMed: 14966139]

Matsui M, Shindo K, Izumi T, Io K, Shinohara M, Komano J, Kobayashi M, Kadowaki N, Harris RS, Takaori-Kondo A. Small molecules that inhibit Vif-induced degradation of APOBEC3G. Virology journal. 2014; 11:122. [PubMed: 24986077]

Max B, Sherer R. Management of the adverse effects of antiretroviral therapy and medication adherence. Clinical infectious diseases : an official publication of the Infectious Diseases Society of America. 2000; 30(Suppl 2):S96–116. [PubMed: 10860894]

Mehle A, Goncalves J, Santa-Marta M, McPike M, Gabuzda D. Phosphorylation of a novel SOCS-box regulates assembly of the HIV-1 Vif-Cul5 complex that promotes APOBEC3G degradation. Genes Dev. 2004; 18:2861–2866. [PubMed: 15574592]

Mehle A, Thomas ER, Rajendran KS, Gabuzda D. A zinc-binding region in Vif binds Cul5 and determines cullin selection. The Journal of biological chemistry. 2006; 281:17259–17265. [PubMed: 16636053]

Mehle A, Wilson H, Zhang C, Brazier AJ, McPike M, Pery E, Gabuzda D. Identification of an APOBEC3G binding site in human immunodeficiency virus type 1 Vif and inhibitors of Vif-APOBEC3G binding. Journal of virology. 2007; 81:13235–13241. [PubMed: 17898068]

Michael NL, Herman SA, Kwok S, Dreyer K, Wang J, Christopherson C, Spadoro JP, Young KK, Polonis V, McCutchan FE, Carr J, Mascola JR, Jagodzinski LL, Robb ML. Development of calibrated viral load standards for group M subtypes of human immunodeficiency virus type 1 and performance of an improved AMPLICOR HIV-1 MONITOR test with isolates of diverse subtypes. Journal of clinical microbiology. 1999; 37:2557–2563. [PubMed: 10405401]

Miyagi E, Opi S, Takeuchi H, Khan M, Goila-Gaur R, Kao S, Strebel K. Enzymatically active APOBEC3G is required for efficient inhibition of human immunodeficiency virus type 1. Journal of virology. 2007; 81:13346–13353. [PubMed: 17928335]

Nathans R, Cao H, Sharova N, Ali A, Sharkey M, Stranska R, Stevenson M, Rana TM. Small-molecule inhibition of HIV-1 Vif. Nature biotechnology. 2008; 26:1187–1192.

Newman EN, Holmes RK, Craig HM, Klein KC, Lingappa JR, Malim MH, Sheehy AM. Antiviral function of APOBEC3G can be dissociated from cytidine deaminase activity. Curr Biol. 2005; 15:166–170. [PubMed: 15668174]

Pan T, He X, Chen B, Chen H, Geng G, Luo H, Zhang H, Bai C. Development of benzimidazole derivatives to inhibit HIV-1 replication through protecting APOBEC3G protein. European journal of medicinal chemistry. 2015; 95:500–513. [PubMed: 25847768]

Pery E, Rajendran KS, Brazier AJ, Gabuzda D. Regulation of APOBEC3 proteins by a novel YXXL motif in human immunodeficiency virus type 1 Vif and simian immunodeficiency virus SIVagm Vif. Journal of virology. 2009; 83:2374–2381. [PubMed: 19109396]

Pery E, Sheehy A, Nebane NM, Brazier AJ, Misra V, Rajendran KS, Buhrlage SJ, Mankowski MK, Rasmussen L, White EL, Ptak RG, Gabuzda D. Identification of a Novel HIV-1 Inhibitor Targeting Vif-dependent Degradation of Human APOBEC3G. The Journal of biological chemistry. 2015

Ptak RG, Gallay PA, Jochmans D, Halestrap AP, Ruegg UT, Pallansch LA, Bobardt MD, de Bethune MP, Neyts J, De Clercq E, Dumont JM, Scalfaro P, Besseghir K, Wenger RM, Rosenwirth B. Inhibition of human immunodeficiency virus type 1 replication in human cells by Debio-025, a novel cyclophilin binding agent. Antimicrobial agents and chemotherapy. 2008; 52:1302–1317. [PubMed: 18212100]

Refsland EW, Stenglein MD, Shindo K, Albin JS, Brown WL, Harris RS. Quantitative profiling of the full APOBEC3 mRNA repertoire in lymphocytes and tissues: implications for HIV-1 restriction. Nucleic acids research. 2010; 38:4274–4284. [PubMed: 20308164]

Russell RA, Pathak VK. Identification of two distinct human immunodeficiency virus type 1 Vif determinants critical for interactions with human APOBEC3G and APOBEC3F. Journal of virology. 2007; 81:8201–8210. [PubMed: 17522216]

Schlapfer E, Fischer M, Ott P, Speck RF. Anti-HIV-1 activity of leflunomide: a comparison with mycophenolic acid and hydroxyurea. Aids. 2003; 17:1613–1620. [PubMed: 12853743]

Schrofelbauer B, Chen D, Landau NR. A single amino acid of APOBEC3G controls its species-specific interaction with virion infectivity factor (Vif). Proceedings of the National Academy of Sciences of the United States of America. 2004; 101:3927–3932. [PubMed: 14978281]

Schumacher AJ, Hache G, Macduff DA, Brown WL, Harris RS. The DNA deaminase activity of human APOBEC3G is required for Ty1, MusD, and human immunodeficiency virus type 1 restriction. Journal of virology. 2008; 82:2652–2660. [PubMed: 18184715]

Setzer B, Lebrecht D, Walker UA. Pyrimidine nucleoside depletion sensitizes to the mitochondrial hepatotoxicity of the reverse transcriptase inhibitor stavudine. The American journal of pathology. 2008; 172:681–690. [PubMed: 18276780]

Sheehy AM, Gaddis NC, Choi JD, Malim MH. Isolation of a human gene that inhibits HIV-1 infection and is suppressed by the viral Vif protein. Nature. 2002; 418:646–650. [PubMed: 12167863]

Smith JL, Bu W, Burdick RC, Pathak VK. Multiple ways of targeting APOBEC3-virion infectivity factor interactions for anti-HIV-1 drug development. Trends in pharmacological sciences. 2009; 30:638–646. [PubMed: 19837465]

Strebel K. HIV accessory proteins versus host restriction factors. Current opinion in virology. 2013; 3:692–699. [PubMed: 24246762]

Tolstonog GV, Deppert W. Metabolic sensing by p53: keeping the balance between life and death. Proceedings of the National Academy of Sciences of the United States of America. 2010; 107:13193–13194. [PubMed: 20647386]

Towner WJ, Xu L, Leyden WA, Horberg MA, Chao CR, Tang B, Klein DB, Hurley LB, Quesenberry CP Jr, Silverberg MJ. The effect of HIV infection, immunodeficiency, and antiretroviral therapy on the risk of hepatic dysfunction. Journal of acquired immune deficiency syndromes. 2012; 60:321–327. [PubMed: 22343179]

Vahey M, Nau ME, Barrick S, Cooley JD, Sawyer R, Sleeker AA, Vickerman P, Bloor S, Larder B, Michael NL, Wegner SA. Performance of the Affymetrix GeneChip HIV PRT 440 platform for antiretroviral drug resistance genotyping of human immunodeficiency virus type 1 clades and viral isolates with length polymorphisms. Journal of clinical microbiology. 1999; 37:2533–2537. [PubMed: 10405396]

Wang QY, Bushell S, Qing M, Xu HY, Bonavia A, Nunes S, Zhou J, Poh MK, Florez de Sessions P, Niyomrattanakit P, Dong H, Hoffmaster K, Goh A, Nilar S, Schul W, Jones S, Kramer L, Compton T, Shi PY. Inhibition of dengue virus through suppression of host pyrimidine biosynthesis. Journal of virology. 2011; 85:6548–6556. [PubMed: 21507975]

Wang X, Wang X, Zhang H, Lv M, Zuo T, Wu H, Wang J, Liu D, Wang C, Zhang J, Li X, Wu J, Yu B, Kong W, Yu X. Interactions between HIV-1 Vif and human ElonginB-ElonginC are important for CBF-beta binding to Vif. Retrovirology. 2013; 10:94. [PubMed: 23988114]

Wei X, Decker JM, Liu H, Zhang Z, Arani RB, Kilby JM, Saag MS, Wu X, Shaw GM, Kappes JC. Emergence of resistant human immunodeficiency virus type 1 in patients receiving fusion inhibitor (T-20) monotherapy. Antimicrobial agents and chemotherapy. 2002; 46:1896–1905. [PubMed: 12019106]

Yamashita T, Kamada K, Hatcho K, Adachi A, Nomaguchi M. Identification of amino acid residues in HIV-1 Vif critical for binding and exclusion of APOBEC3G/F. Microbes Infect. 2008; 10:1142–1149. [PubMed: 18603011]

Zameitat E, Gojkovic Z, Knecht W, Piskur J, Loffler M. Biochemical characterization of recombinant dihydroorotate dehydrogenase from the opportunistic pathogenic yeast Candida albicans. The FEBS journal. 2006; 273:3183–3191. [PubMed: 16774642]

Zhang H, Yang B, Pomerantz RJ, Zhang C, Arunachalam SC, Gao L. The cytidine deaminase CEM15 induces hypermutation in newly synthesized HIV-1 DNA. Nature. 2003; 424:94–98. [PubMed: 12808465]

Zuo T, Liu D, Lv W, Wang X, Wang J, Lv M, Huang W, Wu J, Zhang H, Jin H, Zhang L, Kong W, Yu X. Small-molecule inhibition of human immunodeficiency virus type 1 replication by targeting the interaction between Vif and ElonginC. Journal of virology. 2012; 86:5497–5507. [PubMed: 22379088]

- We screen over 300,000 compounds and identify redoxal as an inhibitor of HIV Vif-APOBEC3G interaction.

- Redoxal is a known inhibitor of dihydroorotate dehydrogenase, an essential enzyme for pyrimidine biosynthesis.

- Redoxal augments APOBEC3G antiviral activity by stabilizing APOBEC3G protein and increasing its levels in HIV virions

- These results identify redoxal as an inhibitor of HIV replication that acts by augmenting APOBEC3G antiviral activity
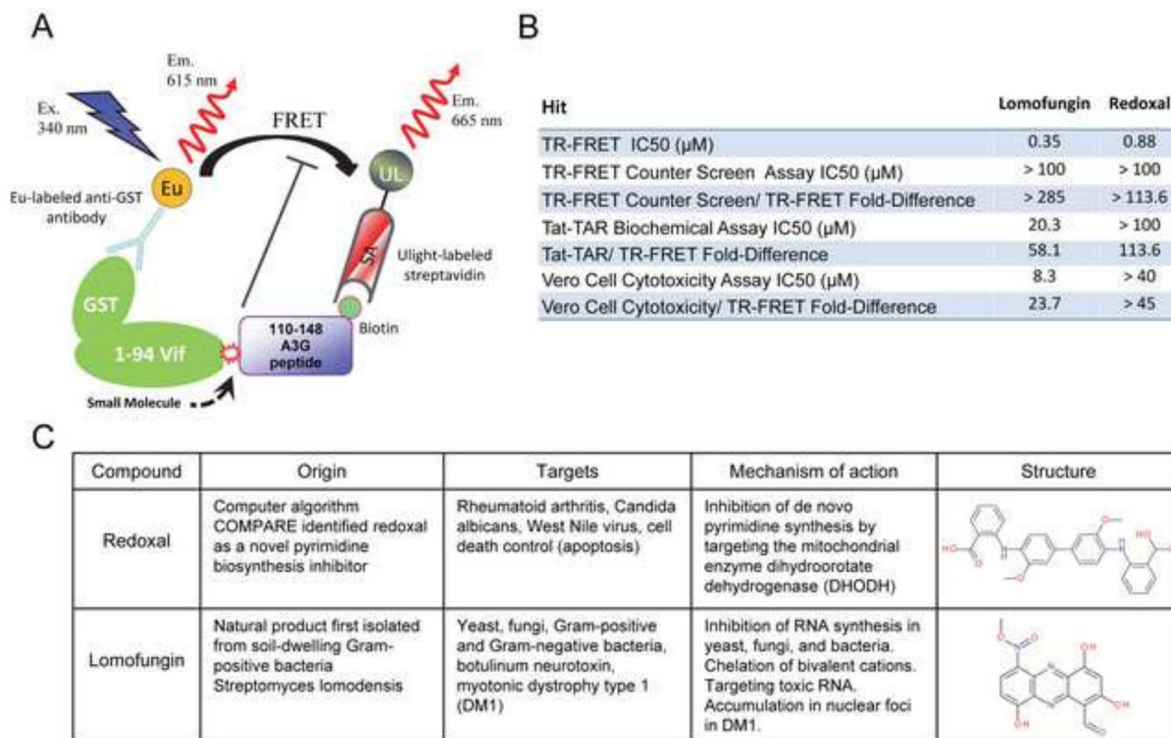
Figure 1. Identification of redoxal and lomofungin as inhibitors of HIV-1 Vif-APOBEC3G interaction in a TR-FRET based assay

A. TR-FRET based assay used to screen for inhibitors of HIV-1 Vif-A3G interaction. The interaction between purified GST-Vif (amino acids 1–94) and biotinylated A3G peptide (amino acids 110–148, a surrogate for the Vif binding site) was detected by Europium (Eu; donor fluorophore)-labeled anti-GST antibody and streptavidin-UL (Ulight; acceptor fluorophore). B. Dose response TR-FRET assay and counter screen testing of compounds redoxal and lomofungin for specificity and activity validation. The z-values calculated for the counter screens and cytotoxicity assays ranged from 0.70 to 0.91. C. Summary of redoxal and lomofungin including targets, known mechanisms of action, and structures.
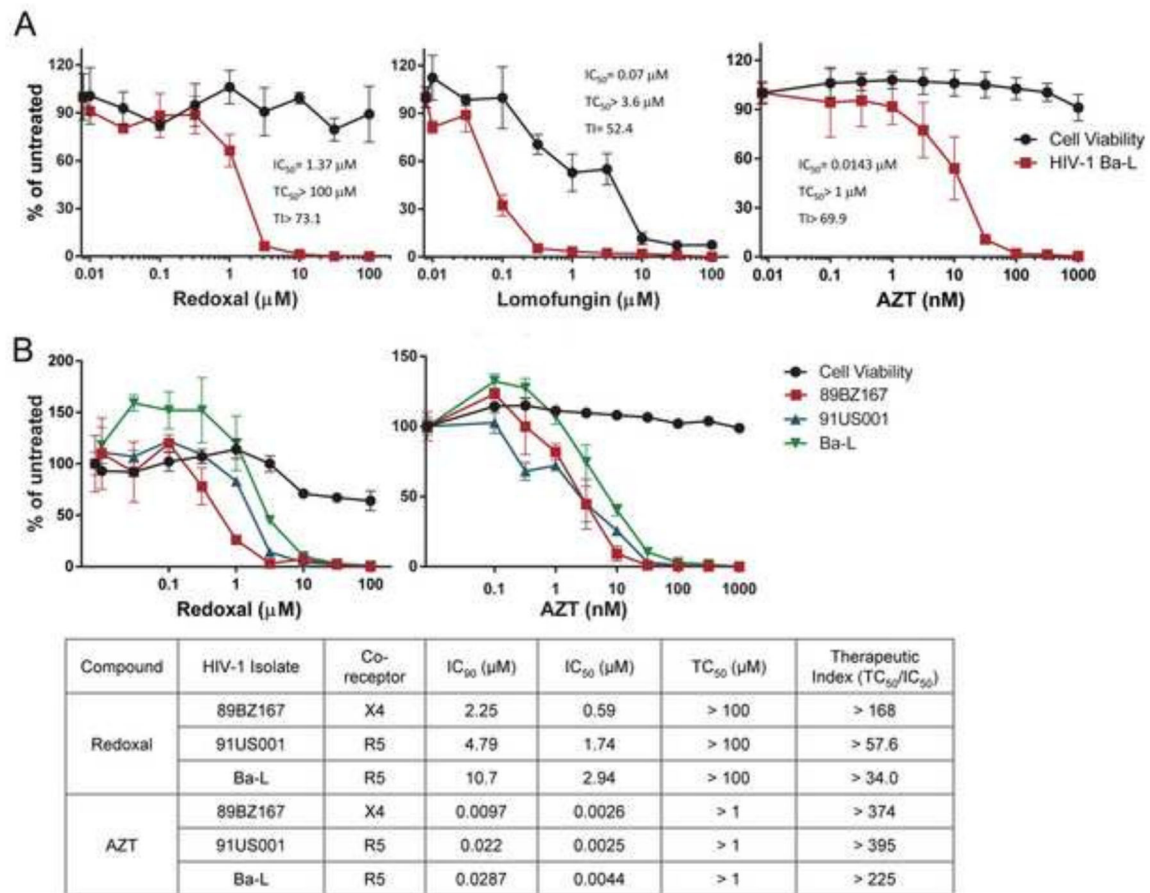
Figure 2. Redoxal and lomofungin inhibit HIV-1 replication in PBMCs

A. Antiviral activity against HIV-1 replication in PBMCs. Redoxal and lomofungin were evaluated in dose-response assays using a high-test concentration of 100 μM and half-log dilutions. AZT was included as a positive control antiviral compound. Treated PBMCs were infected with HIV-1$_{Ba-L}$ isolate and 7 days post-infection virus replication and cell viability were measured by RT and MTS assays, respectively. Calculated values of the IC_{50}, TC_{50}, and therapeutic index of the compounds are shown. B. Redoxal exhibits broad antiviral activity against replication of diverse HIV-1 isolates in PBMCs. Antiviral activity against replication of three HIV-1 isolates in PBMCs. Redoxal was evaluated in dose-response assays using a high-test concentration of 100 μM and half-log dilutions. Treated PBMCs were infected with three HIV-1 isolates: Ba-L, 89BZ167, and 91US001. Seven days post-infection virus replication and cell viability were measured by RT and MTS assays, respectively. AZT served as the positive control antiviral compound. Calculated values of tested compounds' IC_{90}, IC_{50}, TC_{50} and therapeutic index are shown. Shown in A and B are percentage of virus replication and cell viability in compound-treated cells relative to untreated controls. Results are representative of 3 independent experiments each done in triplicate (upper panel; means of triplicate samples from independent wells ± SD).
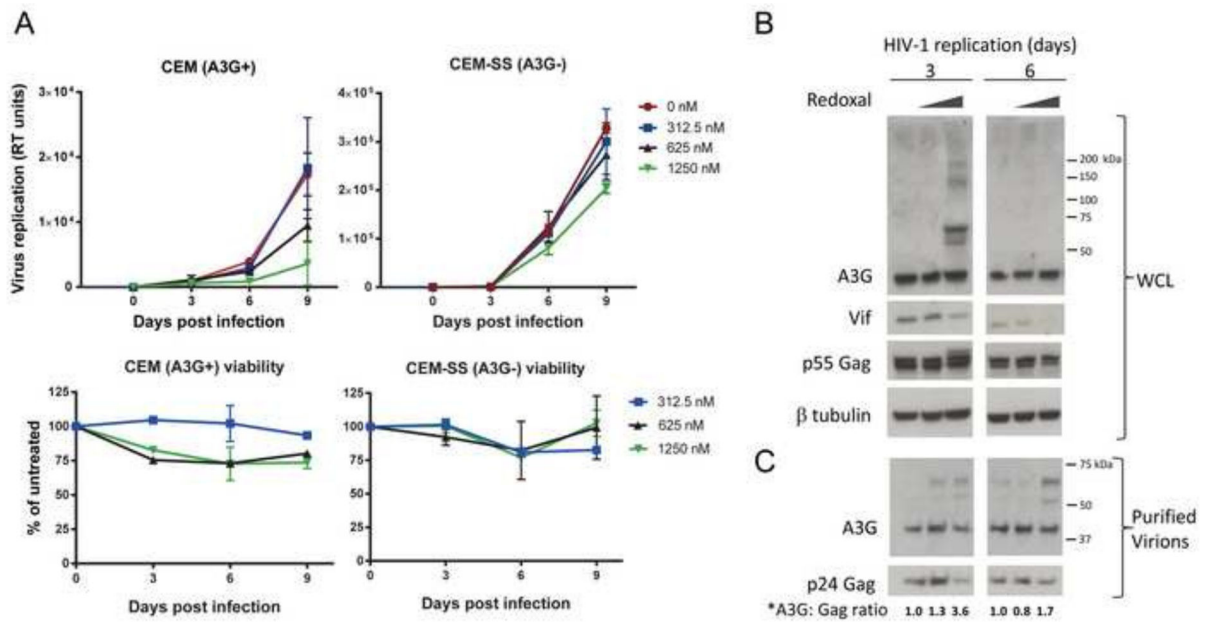
Figure 3. Redoxal inhibits HIV-1 replication in an A3G-expressing T cells

A. HIV-1 spreading infection in redoxal-treated T cells. CEM and CEM-SS T cells were infected with HIV-1$_{NL4-3}$ and 3 h post-infection cells were treated with 0, 312.5, 625, and 1250 nM redoxal. Virus production and cell viability of treated cells was tested at 3, 6, and 9 days post-infection by RT and CellTiter-Glo assays, respectively. HIV-1 replication is shown in RT units. Percentage of cell viability in redoxal-treated cells is relative to untreated controls (means of duplicate samples from independent wells ± SD). B. Redoxal induces the appearance of high molecular weight forms of A3G protein in HIV-1 infected CEM T cells. Infected cells treated with 0, 625, or 1250 nM redoxal were lysed 3 and 6 days post infection. Endogenous A3G, Vif, p55^{Gag}, and β-tubulin protein levels in infected cell lysates were analyzed by Western blotting. WCL: Whole Cell Lysates. C. Redoxal induces the appearance of high molecular weight forms of A3G protein incorporated into HIV-1 virions. Virions collected 3 and 6 days post infection were normalized for equivalent RT units and purified through 20% sucrose. A3G and p24 ^{Gag} protein levels in virion lysates were detected by Western blotting. *Values shown below A3G and p24 ^{Gag} blots represent relative levels of virion-associated A3G protein in virions produced in HIV-1 infected cells treated with redoxal were determined by densitometry of bands using ImageJ software and normalization to untreated cells (DMSO control).
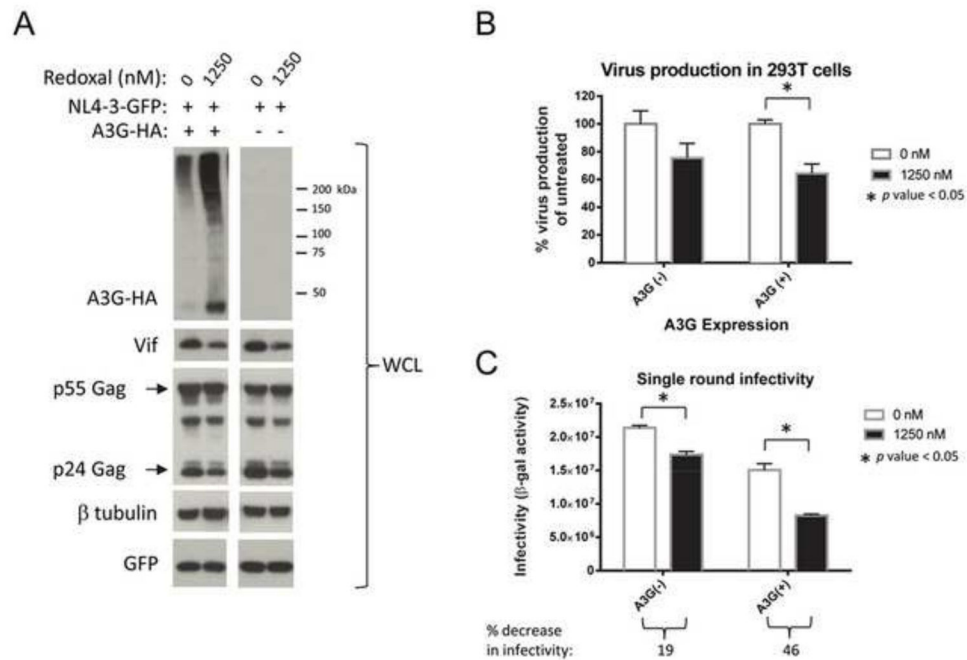
Figure 4. Redoxal attenuates virus production and infectivity

A. Redoxal increases A3G protein levels in HIV-1 producer cells. 293T cells were co-transfected with 0.1 μg A3G-3xHA and 1 μg pNL4-3GFP Env HIV-1 plasmids using VSV-G envelope glycoprotein for pseudotyping. Five hours post-transfection, the media was replaced with fresh media supplemented with DMSO or 1250 nM redoxal. At 40 h post transfection, supernatants containing virus were collected and producer cells were lysed. A3G, Vif, p24$^{\mathrm{Gag}}$, GFP and β-tubulin protein levels in producer cell lysates were analyzed by Western blotting B. Redoxal decreases viral particles produced independently of A3G expression. Virus production from DMSO- and redoxal-treated cells was quantified by RT assay. Percentage of virus production is relative to virus production of untreated producer cells. Results representative of two independent experiments each performed in duplicate. C. Redoxal attenuates infectivity of viruses produced from cells expressing A3G proteins. TZM-bl reporter cells were infected with viruses corresponding to 4,000 RT units. Infectivity was measured 48 h post infection. Results are representative of two independent experiments each done in triplicate. The percentage decrease in the infectivity of viruses produced from redoxal-treated cells compared to controls is shown below the graph. Shown in B and C are means ± SD of duplicate samples from independent wells (p-values from student's t-test).
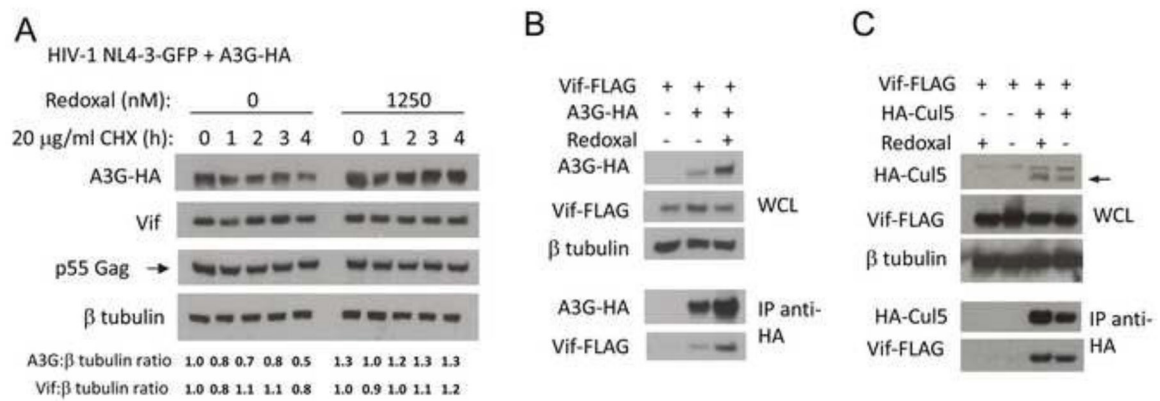
Figure 5. Redoxal augments A3G protein stability without disrupting Vif interaction with A3G, or Cul5

A. Redoxal augments A3G protein stability in cells expressing HIV-1 Vif. 293T cells were co-transfected with 100 ng A3G-3xHA and 1000 ng pNL4-3GFP Env HIV-1 plasmids. At 5 h post transfection, the media was replaced with media supplemented with 1250 nM redoxal. After 36 h of redoxal treatment, CHX was added. At the time intervals indicated after CHX treatment cells were lysed and A3G, Vif, p55^{Gag}, and β-tubulin protein levels were analyzed. Values shown below the blots represent relative A3G or Vif protein levels in treated cells determined by densitometry using ImageJ software and normalization to A3G or Vif protein levels in untreated cells (DMSO control). B. Redoxal does not disrupt Vif-A3G interaction in 293T cells. 293T cells were co-transfected with 2000 ng pNLA1.Vif-FLAG and 300 ng A3G-3xHA or pCDNA3.1 (empty vector). The cells were then treated with 1250 nM redoxal for 40 h. At 48 h post transfection, cells were lysed and subjected to protein analysis. Western blot of cell lysates or anti-HA co-immunoprecipitated proteins were probed using anti-Vif and anti-HA antibodies. C. Redoxal does not affect Vif-Cul5 interaction in co-immunoprecipitation assays. 293T cells were co-transfected with 2000 ng pNLA1.Vif-FLAG and either 4000 ng HA-Cullin 5 or pCDNA3.1 (empty vector) expression constructs. Transfected cells were treated with DMSO or 1250 nM redoxal for 40 h. Cells were lysed 48 h after transfection. Cell lysates or anti-HA co-immunoprecipitated proteins were analyzed using anti-Vif and anti-HA antibodies.
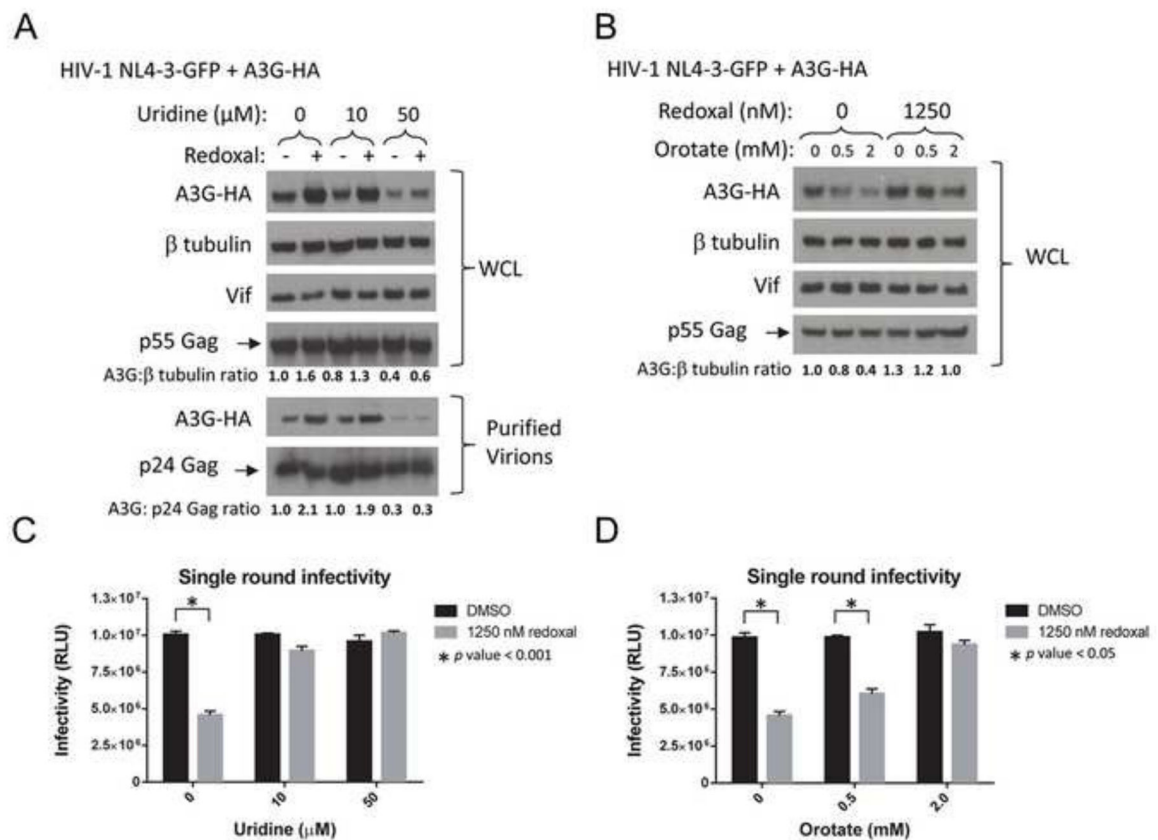
Figure 6. Redoxal increases cellular A3G protein levels by inhibiting *de novo* pyrimidine biosynthesis

A. Redoxal increases A3G protein levels in virus producer cells and newly produced virions while uridine supplementation reverses these effects of redoxal. 293T cells were co-transfected with 100 ng A3G-3xHA and 1000 ng pNL4-3GFP Env HIV-1 plasmids. At 5 h post transfection, the media was replaced with fresh media supplemented with DMSO or 1250 nM redoxal and supplemented with increasing doses of uridine (0, 10, or 50 μM). At 40 h post transfection, supernatants containing virus were collected, producer cells were lysed, and A3G, Vif, p55 Gag, and β-tubulin protein levels in producer cell lysates were detected by Western blotting (upper panels). Lower panels: A3G incorporation into virions produced from cells analyzed in the upper panels. Virions normalized for equivalent RT units were purified through 20% sucrose and A3G and p24 Gag protein levels in virion lysates were detected by Western blotting (lower panels). Results are representative of two independent experiments.. B. Redoxal increases cellular A3G protein expression in virus producer cells while orotate supplementation reverses this effect of redoxal. 293T cells were co-transfected with 100 ng A3G-3xHA and 1000 ng pCDNA3.1 (empty vector) plasmids. At 5 h post transfection, the media was replaced with fresh media supplemented with DMSO or 1250 nM redoxal and supplemented with increasing doses of orotate (0, 0.5, or 2 mM). At 40 h post transfection, cells were lysed. A3G and β-tubulin protein levels in cell lysates were analyzed by Western blotting. Results are representative of two independent experiments. Values shown below blots in A and B represent relative A3G protein levels in treated cells determined by densitometry using ImageJ software and normalization to A3G protein levels

in untreated cells (DMSO control). C. and D. Redoxal attenuates infectivity of VSV-G pseudotyped NL4-3GFP Env viruses produced in A3G-expressing 293T cells, while uridine and orotate supplementation reverse this effect of redoxal. TZM-bl reporter cells were infected with viruses corresponding to 4,000 RT units. Infectivity was measured 48 h post infection. Results are representative of two independent experiments each done in triplicate. Shown in C and D are means ± SD of triplicate samples from independent wells (p-values from student's t-test).
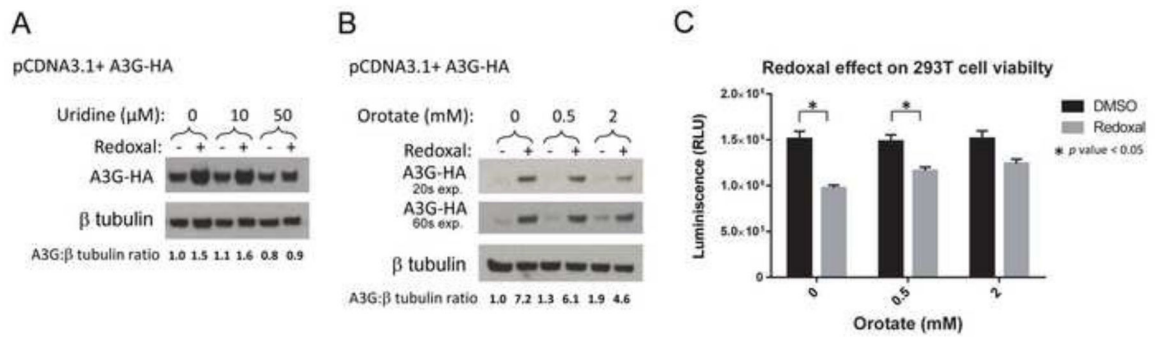
Figure 7. Uridine and orotate supplementation reverse the effects of redoxal on A3G protein levels in the absence of Vif

A. Uridine supplementation diminishes redoxal-induced augmentation of cellular A3G protein levels in the absence of HIV-1 Vif. 293T cells were co-transfected with 100 ng A3G-3xHA and 1000 ng pCDNA3.1 (empty vector) plasmids. At 5 h post transfection, the media was replaced with fresh media supplemented with DMSO or 1250 nM redoxal and increasing doses of uridine (0, 10, or 50 μM). At 40 h post transfection, cells were lysed. A3G and β-tubulin protein levels in cell lysates were analyzed by Western blotting. Results are representative of two independent experiments. B. Orotate supplementation diminishes redoxal-induced augmentation of cellular A3G protein levels in the absence of HIV-1 Vif. 293T cells were co-transfected with 100 ng A3G-3xHA and 1000 ng pCDNA3.1 (empty vector) plasmids. At 5 h post transfection, the media was replaced with fresh media supplemented with DMSO or 1250 nM redoxal and supplemented with increasing doses of orotate (0, 0.5, or 2.0 mM). At 40 h post transfection, cells were lysed. A3G and β-tubulin protein levels in cell lysates were analyzed by Western blotting. A3G blots are shown for two exposure times (20 and 60 sec). Results are representative of two independent experiments. Values shown below blots in A and B represent relative A3G protein levels in treated cells determined by densitometry using ImageJ software and normalization to A3G protein levels in untreated cells (DMSO control). C. Pyrimidine depletion by redoxal decreases cell viability. Viability of treated cells described in Fig. 8B was measured using CellTiter-Glo® Luminescent cell viability assay. Results are representative of two independent experiments. Shown are means ± SD of duplicate samples from independent wells (p-values from student's t-test).
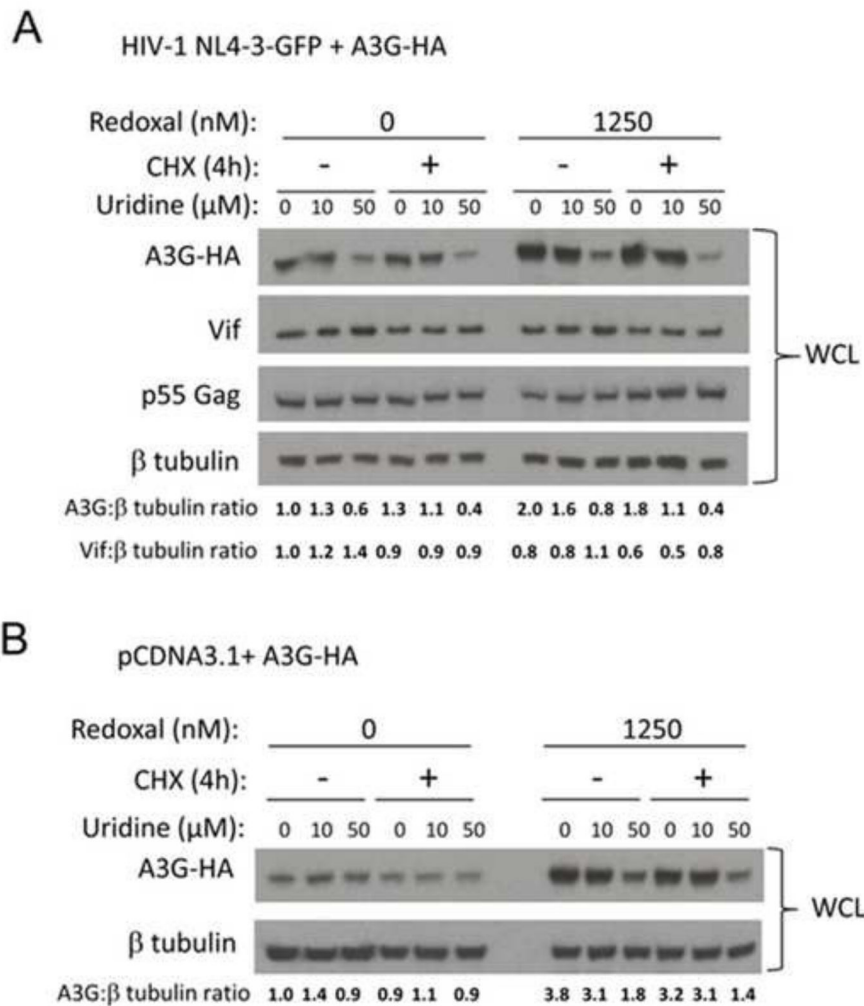
Figure 8. Pyrimidine depletion induced by redoxal increases A3G protein stability

A. Pyrimidine depletion by redoxal augments A3G protein stability in virus producer cells. 293T cells were co-transfected with 100 ng A3G-3xHA and 1000 ng pNL4-3GFP Env HIV-1 plasmids. At 5 h post transfection, the media was replaced with fresh media supplemented with DMSO or 1250 nM redoxal and supplemented with uridine (0, 10 or 50 μM) for 36 h followed by CHX treatment. At 0 and 4 h post CHX treatment, cells were lysed. A3G, Vif, p55 Gag, and β-tubulin protein levels in producer cell lysates were detected by Western blotting. B. Pyrimidine depletion by redoxal augments A3G protein stability in the absence of Vif. 293T cells were co-transfected with 100 ng A3G-3xHA and 1000 ng pCDNA3.1 (empty vector) plasmids. At 5 h post transfection, the media was replaced with fresh media supplemented with DMSO or 1250 nM redoxal and supplemented with uridine (0, 10 or 50 μM) for 36 h followed by CHX treatment. At 0 and 4 h post CHX treatment, cells were lysed. A3G and β-tubulin protein levels in cell lysates were analyzed by Western blotting. Results are representative of two independent experiments. Values shown below blots in A and B represent relative A3G or Vif protein levels in treated cells determined by densitometry using ImageJ software and normalization to A3G or Vif protein levels in

untreated cells (DMSO control). Results shown in A and B are representative of two independent experiments.